NRF2 through RPS6 activation is related to anti-HER2 drug resistance in HER2-amplified gastric cancer

Valentina Gambardella[1*], Francisco Gimeno-Valiente[1*], Noelia Tarazona[1, 2], Carolina Martinez Carpaglini[3], Desamparados Roda[1, 2], Tania Fleitas[1], Pablo Tolosa[1], Juan Miguel Cejalvo[1], Marisol Huerta[1], Susana Roselló[1, 2], Josefa Castillo[1, 2, 4,5] and Andrés Cervantes1[1,2, 5].

[1] Dept. Medical Oncology. INCLIVA Biomedical Research Institute. University of Valencia. Valencia, Spain.
[2] CIBERONC. Network of Biomedical Research. Instituto de Salud Carlos III. Spain.
[3] Dept. of Pathology. INCLIVA Biomedical Research Institute. University of Valencia. Valencia, Spain.
[4] Dept. of Biochemistry and Molecular Biology, University of Valencia. Valencia, Spain.

[*]Valentina Gambardella and Francisco Gimeno-Valiente contributed equally to this article.

[5]Corresponding authors: Josefa Castillo and Andrés Cervantes contributed equally to this article as corresponding authors. Dept. Medical Oncology. INCLIVA Biomedical Research Institute. University of Valencia. Blasco Ibáñez 17; 46010 Valencia, Spain. Phone: +34961973543; Fax:+34961973982
Email: pepa.castillo@uv.es and andres.cervantes@uv.es

Running title: NRF2-RPS6 and anti-HER2 resistance in HER2+ gastric cancer.

Financial support: This study was supported by grants from the Instituto de Salud Carlos III (Health Institute) (PI18/01909; PI18/01508).
VG was funded by ESMO 2014 fellowship program, and by Rio Hortega contract CM18/00241 from the Carlos III Health Institute; NT was funded by Rio Hortega contract CM15/00246 from the Carlos III Health Institute; DR was funded by Joan Rodes contract 16/00040 from the Carlos III Health Institute; TF was funded by Joan Rodes contract 17/00026 from the Carlos III Health Institute.

The authors declare no potential conflicts of interest.

Translational Relevance

HER2 amplification is detectable in about 7-34% of advanced gastric cancer patients. In combination with platinum-based chemotherapy, trastuzumab has demonstrated therapeutic efficacy. However, the clinical benefit derived from this approach is limited, due to primary and acquired resistance. Moreover, no other anti-HER2 agents have demonstrated relevance in first-line treatment or beyond progression. Herein we show that NRF2 activation through RPS6 is related to resistance to both lapatinib and trastuzumab in *HER2* amplified gastric cancer models. Inhibition of RPS6 and NRF2 reduces cell viability and tumor growth *in vitro* and *in vivo.* In a cohort of *HER2*-amplified GC patients, high NRF2 expression predicted worse response to trastuzumab. This study suggests that RPS6-NRF2 inhibition could be a potential novel therapeutic strategy to overcome resistance in *HER2*-amplified gastric cancer.

Abstract

Purpose: Despite the clinical advantage of the combination of trastuzumab and platinum-based chemotherapy in HER2-amplified tumors, resistance will eventually develop. The identification of molecular mechanisms related to primary and acquired resistance is needed.

Experimental Design: We generated lapatinib- and trastuzumab-resistant clones deriving from two different *HER2*-amplified GC cell lines. Molecular changes such as protein expression and gene expression profile were evaluated to detect alterations which could be related to resistance. Functional studies *in vitro* were corroborated *in vivo*. The translational relevance of our findings was verified in a patient cohort.

Results: We found RPS6 activation and NRF2 to be related to anti-HER2 drug resistance. RPS6 or NRF2 inhibition with siRNA reduced viability and resistance to anti-HER2 drugs. In knockdown cells for RPS6, a decrease of NRF2 expression was demonstrated, suggesting a potential link between these two proteins. The use of a PI3K/TORC1/TORC2 inhibitor, tested *in vitro* and *in vivo*, inhibited pRPS6 and NRF2 expression and caused cell and tumor growth reduction, in antiHER2 resistant models. In a cohort of HER2-amplified patients treated with trastuzumab and chemotherapy, a high level of NRF2 at baseline corresponds with worse progression-free survival (PFS).

Conclusions*:* NRF2 through PI3K/AKT/mTOR/RPS6 pathway could be a potential effector of resistance to anti-HER2 drugs in our models. RPS6 inhibition decreases NRF2 expression and restores sensitivity in HER2-amplified gastric cancer *in vitro* and *in vivo*. High NRF2 expression in gastric cancer patients predicts resistance to treatment. RPS6 and NRF2 inhibition could prevent resistance to anti-HER2 drugs.

Introduction

Human epidermal growth factor receptor 2 (HER2) is one of the best-characterized targetable alterations in solid tumors. (1,2) Among locally advanced or metastatic GC, HER2 is amplified in about 7-34% of patients. (3) Despite a clear improvement in overall survival reported with the use of trastuzumab in combination with platinum-based chemotherapy (4), resistance is a common event (5). Furthermore, other anti-HER2 agents, tested as first-line treatment or beyond progression, achieved disappointing results (6-9) Both tumor heterogeneity and some biological features should be studied for their role in this lack of clinical benefit. (10,11)

Recently NRF2 has been described as a crucial stress response mediator in solid tumors (12). Its activation confers inducible resistance to xenobiotic and oxidative stress (13). In non-small cell lung cancer and pancreatic cancer, high NRF2 levels have recently been related to poor prognosis (14,15). This phenomenon is due not only to chemo/radio-resistance but also to aggressive proliferative phenotypes probably induced by NRF2 (16,17). In gastric cancer NRF2 expression was retrospectively identified as a potential factor of resistance to 5-fluorouracil (18). The mechanisms by which NRF2 promotes cell proliferation are not well understood (19). Under conditions of enhanced proliferation, such as active phosphatidylinositol 3-kinase (PI3K) signaling, NRF2 was shown to augment the expression of metabolic genes that assist in driving proliferative programs (20). The PI3K/AKT/mTOR pathway is commonly deregulated in solid tumors, either by constitutive activation of receptor tyrosine kinases (21) or by inactivation of its repressor PTEN (22). mTOR, which regulates cell growth and proliferation, exists in two distinct protein complexes, mTOR complex1 (mTORC1) and mTOR complex2 (mTORC2) (23). The best-characterized mTORC1 substrates are ribosomal protein S6 kinase (S6K) and the eukaryotic translation initiation factor 4E-binding protein (4E-BP) (24). Activation of S6K and its substrate, ribosomal protein S6 (RPS6), is recognized as an emerging factor in the development of several tumors (25). Ribosomal proteins are moreover described as convergent points of activation of the MAPKK and PI3K/AKT/mTOR signaling pathways (26,27).

The PI3K/AKT/mTOR pathway could occasionally promote cell survival through activation of the nuclear translocation of nuclear factor erythroid 2-related factor 2 (NRF2) (28). Previous studies using several cancer cell lines reported that PI3K and AKT functions are required for NRF2 activation (29). Recently NRF2 has been regarded as one of the main orchestrators of the cellular antioxidant response (12), inducing resistance to chemotherapy (30). Nevertheless, its role in resistance to targeted agents is not yet as well explored as its relation with RPS6.

In the present study we have explored possible mechanisms related to anti-HER2 drug resistance in HER2 amplified gastric cancer models *in vitro* and *in vivo*. We identified a novel role of RPS6, a downstream effector of PI3K/AKT/mTOR pathway, and NRF2 in resistance to anti-HER2 agents in gastric cancer.

Material and methods

Cell lines and chemicals

Human gastric cancer cell lines NCI-N87 and OE19 were obtained from the American Type Culture Collection (ATCC) and the European Collection of Authenticated Cell Cultures (ECACC)-Sigma respectively. Cells were cultured in RPMI 1640 (Thermo Fisher Scientific), supplemented with 10% FBS (Gibco) and 1x penicillin/streptomycin (Gibco). Lapatinib, pimasertib, GSK2126458 (GSK458), saracatinib, everolimus and ly294002 were purchased from Selleck Chemicals. Stock solution was prepared in DMSO, aliquoted and stored at -20ºC. Trastuzumab was obtained from Roche and diluted with phosphate-buffered saline (PBS)

Generation of anti-HER2 drug-resistant cell lines

Derivatives of both OE19 and NCI-N87 lines resistant to HER2-targeted therapies were obtained. Cells were treated with gradually increasing doses starting with IC_{50} dose. Lapatinib dose was progressively increased every 2-3 weeks over a period of 4-5 months until resistant clones emerged. The final lapatinib concentration reached was 1 µmol/L for the OE19 cells and 0.05 µmol/L for the NCI N87 cells. The trastuzumab-resistant model was performed using NCI N87 cells, reaching a final concentration of 1000 µg/ml at the end of this period. OE19 did not present a clear sensitivity to trastuzumab. Each single clone was picked with cloning cylinders (Sigma) and expanded in culture medium containing their specific resistant dose. Parental and resistant cell line authentication was performed by short tandem repeat analysis. All cells were also screened for the presence of mycoplasma before use. The experiments were performed less than 2 months after thawing early passage cells.

Cell growth assays

Cells ($4x10^3$ cells) were seeded in 96-well plates and allowed to adhere overnight. For cell proliferation analysis, viable cells were quantified every 24 h after transfection with siRNAs using MTT reagent 3-[4.5-dimethylthiazol-2yl]-2.5-diphenyl- tetrazolium bromide); Sigma) according to the manufacturer's protocol. In cytotoxicity analysis, cells were treated with the indicated compound with or without siRNA transfection and incubation was continued for an additional 72 hours. Cell viability was determined by MTT. Proliferation or inhibition of proliferation was calculated relative to untreated controls. Each assay was carried out at least in triplicate. The results were finally analyzed with Graphpad to calculate viability and IC_{50} using a log (inhibitor) versus response-variable slope model.

Protein extraction and immunoblotting assays

Whole-cell protein extracts were prepared using RIPA buffer (50 mM Tris-HCl pH 7.5, 150 mM NaCl, 0.1% SDS, 1% Triton x-100, 0.5% deoxycholic acid sodium salt (w/v)) supplemented with 2ul/ml protease inhibitor cocktail (Sigma) and 10ul/ml phosphatase inhibitor cocktail (Sigma). Samples were sonicated and centrifuged at 14,000 xg speed for 20 min at 4ºC. The protein concentration was quantified by a BCA protein assay kit (Thermo Scientific). Nuclear fractions were prepared using Nuclear Extraction kit (Active motif) according to the manufacturer's instructions. Proteins were separated on 10% SDS-polyacrylamide gels, transferred onto a nitrocellulose membrane and incubated with

primary antibodies (Supplementary Table S1). Immunoreactive bands were recognized using peroxidase-conjugated secondary antibody (DAKO). Immunoblots were visualized using the "ECL Western Blotting detection kit" reagent (GE Healthcare) and the ImageQuant LAAS 400 (Healthcare Bio-Sciences) system.
A human Phospho-RTK signaling antibody array kit (Cell signaling, 7982) was used to measure the relative levels of phophorylation for 28 receptor tyrosine kinases and 11 important signaling nodes. 250 µg of protein was used and the array was handled following the manufacturer's protocol.

RNA extraction and reverse transcription-quantitative PCR

RNA isolation, retrotranscription to cDNA and qPCR (RT-qPCR) were performed as previously described (31). Briefly, RNA concentration and purity was determined with Nanodrop and RNA integrity with Bioanalyzer 2100 (Agilent Technologies). A total of 500ng of RNA were retrotranscribed to cDNA using The "High-capacity cDNA Reverse Transcription Kit" (Applied Biosystems). A real time PCR (qPCR) was performed using iTaq Universal SYBR Green Supermix (Bio-Rad) on the "QuantStudio 5 Real-Time PCR System" (Applied Biosystems). All reactions were performed in triplicate. A commercial primer was used to analyze RPS6 gene expression (qHsaCID0038051, Bio-Rad). The rest of the primers, obtained from the PrimerBank database (32) are shown in Supplementary Table S2. Gene expression levels for each amplicon were calculated using 2^-ΔCt method.

Expression profiling analysis by microarray

cDNA from the parental OE19 cell line and its derivative resistant clones LR1OE and LR2OE was synthesized and hybridized to the Affymetrix Clariom S Human array. Data were analyzed and statistically filtered using Partek Genomics Suite v6.6 software. Input files were normalized with the robust multi-chip average (RMA) algorithm for gene array. To narrow the list of relevant genes, a restrictive filtering algorithm was applied using a combined criterion, which required both a fold change absolute value of two or higher and a statistical significance of p<0,005 between subgroups. Each dataset was derived from three biologically independent replicate samples. A Benjamini-Hochberg step-up false discovery rate procedure was also used with a final maximum FDR value of 0.005. Functional annotation clustering of differentially expressed genes was also performed using the Pathway Studio v10 (Elsevier) (Supplementary Table S3).

Transfection with small interfering RNA

The small interfering RNA (siRNA) directed against human RPS6 (SI00708008) or Universal Negative Control (1027310) was purchased from Qiagen. siRNA against NRF2 (EHU093471) was bought from Sigma. Cells were transfected using Lipofectamine RNAiMAX (Invitrogen) according to the manufacturer's instructions. Final concentration of the siRNAs was 20 nmol/L.

Xenograft tumor models

Female immunodeficient SCID mice were purchased at 6 weeks old (Charles River Laboratory). Animal care was in compliance with Spanish and European Community (E.C. L358/1 18/12/86) guidelines on the use and protection of laboratory animals and all procedures were approved by the local ethics committee (2018/VSC/PEA/0101). Mice

were acclimatized for two weeks before being injected with cancer cells and then caged in groups of five under controlled conditions (12 h light-dark cycle; room temperature 20ºC - 22ºC; humidity 55%–60%). A total number of 2 x 10^6 cells in 300 μL of Matrigel (BD Biosciences): PBS (1:1) were subcutaneously injected to the dorsal flank of mice. Once tumors reached a palpable size, mice were treated with 75mg/kg lapatinib by orogastric gavage and 1.5mg/kg GSK458 by i.p. injection given on alternate days. Tumor size was measured twice weekly, and the tumor volume was calculated using the formula: V=1/2(length x width^2) (mm3). When the maximum diameter permitted by the animal care guidelines of our institute was achieved, the mice were euthanized, and each tumor was processed to obtain paraffin and frozen samples.

Immunostaining

Immunohistochemistry staining was performed on the formalin-fixed paraffin-embedded tissue of 31 gastric cancer patients. Sections (2μm) were cut, deparaffinized with xilol and rehydrated using ethanol at 90%, 80% and 70%. After washing in water, the slides were autoclaved for 3 min at 1.5 atmospheres in sodium citrate buffer (pH=6) for antigen retrieval. Endogenous peroxidase activity was blocked with hydrogen peroxidase for 5 min at room temperature. Slides were incubated with pRPS6 ser235/236 (clone D57.2.2E, 1:400, Cell Signaling Technology) or NRF2 (clone EP1808Y, 1:100, Abcam) for 45 min at room temperature. Antibody detection was performed using the Dako Real EnVision HRP Rabbit/Mouse K5007 (Dako) and 3.3' diaminobenzidine (Dako). The slides were also counterstained with hematoxylin chromogen (Dako). The resulted immunostained and H&E slides were examined by a dedicated pathologist. The pRPS6 staining intensity and the proportion of positive cells were recorded using semi-quantitative scores as described by Kim SH et al (33) and Chen B et al (34). In the first, the proportion of positive cells was classified into one of five categories (1: 0%-5%, 2: 5%– 25%, 3: 26%–50%, 4: 51%–75%, or 5: 75%-100%). In the second, a four-tiered scale was used to classify the proportion of positive cells (0: no tumor cell positivity, 1: 0%-10%, 2: 10%-50% or 3: 50%-100%). In both protocols, the staining intensity was classified as 1 (weak), 2 (moderate), or 3 (strong). Finally, both score parameters were multiplied. According to Kim SH et al, cases with a final score of 1 to 4 were considered "low pRPS6", and cases with 5 to 15 "high pRPS6". Using the Chen B et al protocol cases were classified as follow: 0-2: negative, 3 to 5: positive moderate, and 6 to 9: positive strong. The NRF2 immunostaining was evaluated following the protocols previously described by Kawasaky Y et al (35) and Tong Y et al (36). In the first, the percentage of positive cells was recorded (0-100%) and the intensity was quantified using a three-value score (0, 1, or 2). In the second protocol, a semi-quantitative score for the percentage of positive cells (0: 0%–25%, 1: 25%– 50%, 2: 50%–75% or 3: 75%-100%) and the staining intensity (0: absence of staining, 1: weak, 2: moderate; and 3: strong) were assigned. Finally, both score parameters were multiplied. According to Kawasaky et al, only cases with scores above the median were considered positive. Using the scale of Tong Y et al, cases with a final score of 9 were defined as "high expression". The presence of nuclear NRF2 immunostaining in more than 10% of tumor cells was also regarded as "high expression".

To perform the immunofluorescent staining of culture cells, 15x10^3 cells were seeded per well in a μ-slide VI plate (Ibidi). After 24 h cells were fixed with a fresh solution of 4% formaldehyde for 12 min at room temperature and blocked/permeabilized with 0.5% Triton X-100 in PBS. Cells were then incubated with NRF2 antibody 1:500 (EP1808Y, abcam) in blocking and permeabilization solution overnight at 4ºC. An anti-rabbit IgG Alexa Fluor 488 (Invitrogen) was used as a secondary antibody at 1/400 dilution. To visualize the nuclei and preserve the signals generated, the cells were stained with Mounting Medium with

DAPI (Qiagen). The fluorescent images were captured using appropriate filters in a confocal spectral Leica SP2 microscope (Leica Microsystems Heidelberg GmbH).

Patient population

Thirty-one patients diagnosed with locally advanced or metastatic HER2-amplified gastric cancer were included in the analysis. HER2 evaluation was performed according to updated guidelines. To be considered positive and susceptible to treatment with trastuzumab, tumors must have presented IHC +++ for HER2. Pathology records were analyzed and all reports were reviewed. Clinical data were extracted from electronic medical records and reviewed retrospectively to collect age, comorbidities, classic prognostic factors such as T, nodal invasion and site of metastasis. IHC assay was performed to verify the presence of the alteration observed in preclinical models. Written informed consent was obtained from all patients in agreement with approved protocols from the ethics committee.

Ethics approval

The study was conducted in accordance with recognized ethical guidelines (Declaration of Helsinki) and it was approved by the INCLIVA institutional review board (Protocol number: 2017/070). Informed consent from all patients was obtained.

Statistical analysis

Data were analyzed using the GraphPad Prism 6.0 software. Results are shown as means and standard error of the mean. The cut-off for statistical significance was set as $p \leq 0.05$. The sensitivity to anti-HER2 drugs of parental cell lines and their respective resistant clones was studied using parametric two-way ANOVA with interaction and Sidak correction, performing a multivariate comparison of means per dose. A parametric two-way ANOVA test was also applied to xenograft models, to evaluate the effect of drugs in combination versus control and lapatinb alone on tumor growth. In this case, a multivariate comparison of means per time point was done with a Benjamini Yekutieli correction.
A two-way ANOVA with Dunnett multiple comparison test was used to evaluate cells treatments. A Student's t-test was used to evaluate the effect of silencing on cell viability
Kaplan-Meier was used to estimate progression-free survival (PFS) among treated patients. Independent sample *t* tests and Pearson´s correlation were used to study the association of pRPS6 with NRF2 as categorical and continuous variables, respectively. All tests were two sided, and a p value 0.05 was considered statistically significant. Descriptive statistics and survival analysis were performed using IBM SPSS Statistics v20. A Pearson test was used to evaluate correlation. Representation of P value: *< 0.05; **< 0.01; *** < 0.001.

Results

PI3K/AKT/mTOR/RPS6 activation and lapatinib-acquired resistance in HER2-amplified gastric cancer cell lines

To explore the possible mechanisms responsible for anti-HER2 drug resistance, we developed lapatinib resistant clones (LROE) derived from OE19, a HER2-amplified GC cell line. Several stable lapatinib-resistant clones were obtained (LROE) and certified. Two of them (LR1OE and LR2OE) were selected for this work. LR1OE and LR2OE cells were discernibly resistant to lapatinib compared with the parental OE19 cell line, as confirmed by their IC_{50} (Fig.1A).

To look for potential molecular changes in resistant cells an RTK ELISA assay was performed. High activation of RPS6 and SRC in resistant cells was recognized (Fig.1B). To further clarify those changes, protein expression and activation were tested by Western Blot. In our lapatinib-resistant models, HER2 expression was preserved, but its activation was found to be slightly less intense than in sensitive cells. SRC and AKT activation was also confirmed (Fig.1C). Despite the RTK ELISA results, increase in ERK activation was detected in resistant cells. Interestingly, RPS6 was significantly activated among all resistant clones (Fig.1C). RPS6 is one of the components of the 40S ribosomal subunit and has been functionally regarded as a regulator of cellular metabolism, cell size, survival and proliferation. Its activation can be related to both MAPK and PI3K/AKT/mTOR pathways, found to be hyperactivated in our resistant model (26,27) (Fig.1C).

NRF2 emerges as a potential actor in lapatinib-acquired resistance

By performing a transcriptomic assay, we noticed statistically significant mRNA changes between the different cell lines. Principal component analysis (PCA) showed that the alteration of the two resistant models was very similar, suggesting the development of a common alteration induced by continuous exposure to lapatinib (Fig. 2A). Clear differences in the expression of 132 genes, 76 up-regulated and 56 down-regulated, were detected between the two resistant clones and the parental cell line (ANOVA, FDR <0.05) (Supplementary Table S3). Unsupervised hierarchical clustering revealed again a robust classification between two different groups, showing that the resistant cell lines had different gene expression to the parental cell line (Fig. 2B). A functional annotation of altered genes showed enrichment in several biological processes linked with cell metabolism and drug response (Fig. 2C). A significant proportion of the most altered genes belong to the ARE-bearing genes, involved in cellular response to oxidative and xenobiotic stress, known to be regulated by NRF2 (37) (Fig. 2D). Altered gene expression was validated by RT-qPCR (Fig. 2E). This transcriptomic assay suggested NRF2 was involved in lapatinib resistance in our experimental model. Moreover, a Western Blot showed a NFR2 overexpression in LR1OE and LR2OE cells, reinforcing the idea of NRF2 involvement in acquired resistance to lapatinib in our model (Fig. 2F).

NRF2 and RPS6 are altered in anti-HER2 acquired resistance across different models

To validate the previous results, we analyzed another HER2-amplified GC cell line, NCI-N87 and developed lapatinib and trastuzumab resistant clones (Fig. 3A). Interestingly LRNCI cells were found to be resistant even to trastuzumab (Supplementary Fig. S1). The persistence of HER2 expression was seen and its activation was higher in trastuzumab-resistant cells (Fig 3B). Importantly, RPS6 expression and activation was also confirmed across these cell lines by Western Blot (Fig 3B). Its activation was higher in TR1NCI. Nevertheless, in LR1NCI, SRC and ERK activation was prominently detected, as was found in the lapatinib-resistant clones derived from OE19. Unlike these models, AKT was not activated in LR1NCI (Fig. 3B). In both lapatinib- and trastuzumab-resistant clones derived from NCI N87, NRF2 increased expression was also confirmed by Western Blot (Fig. 3C). These results suggest that NRF2 plays a relevant role in resistance to anti-HER2 drugs. Once activated, NRF2 moves into the nucleus, where it triggers its target genes. An immunofluorescence assay demonstrated the nuclear presence of NRF2 in lapatinib- and trastuzumab-resistant clones, suggesting its activation across different resistant models (Fig. 3D). A subcellular fractionation confirmed the prevalence of the nuclear expression among resistant cells (Supplementary Fig. S2).

Inhibition of PI3K/AKT/mTOR/RPS6, but not SRC or MEK, reduces cell viability in HER2-resistant cell lines

A panel of targeted drugs, such as pimasertib, everolimus, GSK458 and saracatinib were tested to evaluate the relevance of the described alteration in conferring resistance to anti-HER2 drugs. Despite the activation of SRC, no significant effect was observed from the use of saracatinib, a potent and specific SRC inhibitor. Everolimus, an mTOR inhibitor, demonstrated a not significant reduction in cell viability. When a MEK inhibitor, pimasertib, was tested, it was possible to observe a slight decrease in viability only in LR2OE and LR1NCI. Remarkably, the use of a dual PI3K/TORC1/TORC2 inhibitor, GSK458, was able to inhibit viability considerably in all models (Fig. 4A), probably due to its capability in inhibiting TORC1, which is supposed to directly activate RPS6 protein (Fig. 4A) (21).
To better define the role of RPS6 on cell viability, siRNAs were used to silence its expression. Interestingly, the proliferation of knockdown cells was significantly reduced versus the control (Fig. 4B), indicating a primary role of RPS6 in cell growth and survival. When silenced RPS6-resistant cells were treated with lapatinib and trastuzumab respectively, a statistically significant reduction of resistance was observed (Fig. 4C). Decreased viability seems to vary proportionally to each RPS6 activation level. This evidence further points to the important role of RPS6 in developing resistance to antiHER2 agents.

Targeting RPS6 activation decreases NRF2 expression in resistant models

It has already been reported that ribosomal proteins increase NRF2 expression through its association with RNA binding proteins (RBPs). To address whether RPS6 could be involved in NRF2 increase. A knockdown of RPS6 was performed. Western Blot analysis highlighted the decrease of NRF2 expression in LR1OE silenced by RPS6 (Fig. 4D). In these cells, decreased expression of the activated genes, such as AKR1C1, AKR1C2, AKR1B10 induced by NRF2 was also detectable, suggesting the functional dependence of NRF2 and RPS6 (Fig. 4D). The impact of increased NRF2 expression was studied by siRNA silencing, observing a significant decrease of cell proliferation in lapatinib- and

trastuzumab-resistant models (Fig. 4E). Interestingly, lapatinib in LR1OE NRF2 knockdown cells was able to reduce viability in a statistically significant way. A slight effect was also observed with trastuzumab when siC and siNRF2 at each doses were compared (Fig. 4F). To evaluate which compound was able to inhibit pRPS6 and NRF2, a panel of drugs were tested, such as LY294002, everolimus, GSK458, pimasertib and lapatinib. Western Blot analysis and quantification suggest an important role in inhibiting both pRPS6 and NRF2 using the dual PI3K/TORC1/TORC2 inhibitor, GSK458 (Fig. 4G). This evidence confirms the link between RPS6 and NRF2, suggesting that a PI3K/TORC1/TORC2 inhibitor may be used to overcome anti-HER2 resistance.

NRF2 via RPS6 activation could be responsible for lapatinib resistance in HER2-amplified gastric cancer *in vivo*

To corroborate our results on NRF2 activation through PI3K/AKT/mTOR/RPS6 and its role in resistance to anti-HER2 therapies, we planned an *in vivo* experiment. LR1OE were subcutaneously implanted in SCID mice that were successively randomized and treated with vector or lapatinib. Once tumors were detectable, the mice treated with lapatinib were randomized to continue treatment or to receive GSK458. As HER2 expression was preserved in our resistant models, lapatinib was maintained over resistant cells *in vivo*. In a previous experiment, parental NCI-N87 and OE-19 cell lines, GSK458 was found to be mildly effective and the combination with lapatinib was no longer able to improve the results obtained with lapatinib single agent *in vitro* (Supplementary Figure S3). However, a significant difference in tumor growth of LR1OE was observed according to the different treatment administered *in vivo*. As expected, there were no differences in tumor growth between control and lapatinib, while tumor growth was significantly reduced when GSK458 was added (Fig. 5A) suggesting the relevant role of GSK48 in resistant models. When tumors achieved the maximum tolerated volume, xenografts were euthanized and the autopsies confirmed that GSK458 was able to significantly reduce tumor growth (Fig. 5B). The analysis of samples performed by Western Blot (Fig. 5C), confirmed that tumors still preserved HER2 expression. AKT activation was also detectable. The cleavage of PARP was observed when the combination was administered. As reported in our *in vitro* assays, pRPS6 and NRF2 were expressed in tumor tissues of xenografts treated with vector and lapatinib (Fig. 5C), suggesting their potential role in resistance, while when GSK458 was used, pRPS6 and NRF2 were no longer detectable. A considerable reduction in the expression of NRF2 target genes was also observed (Fig. 5D). These results highlighted the relation between RPS6 and NRF2, namely that NRF2 expression decreases when pRPS6 is inhibited.

RPS6 and NRF2 predict resistance to trastuzumab in HER2-amplified gastric cancer patients

We retrospectively analyzed a cohort of patients diagnosed with HER2-amplified locally advanced or metastatic GC (Supplementary Table S4). The aim was to explore the clinical relevance of the findings previously identified in our cell-resistant models. HER2 IHC was evaluated by a dedicated pathologist. Only patients with a high expression by IHC of HER2 (3+) were considered for this study. Electronical medical records and pathology reports were reviewed and finally 31 patients were considered eligible. IHC analyses of pRPS6 and NRF2 over paraffin-embedded samples were performed to verify the role of NRF2 and

PIK3/AKT/mTOR/RPS6 activation in diagnosis (33-36). pRPS6 expression was high in 70.1% (22/31) patients, moderate in 12.9% (4/31) and low in 16.1% (5/31). NRF2 expression was high in 32.2% (10/31) and low in 67.7% (21/31). pRPS6 hyperexpression was not always correlated with increase in NRF2 (r= 0,21, *p*= 0,27). However, in 9 out of 10 cases with high NRF2 expression, high expression of pRPS6 was also observed (Fig 6A). Progression-free survival was calculated for all patients who had received first-line treatment with trastuzumab and chemotherapy (21 patients). Median time to progression was 9 months for the whole group (2-34 months). Patients with high NRF2 expression (n=9) at baseline presented poor prognosis with a median time to progression of only 4 months whereas patients with low NRF2 expression (n=12) did better with a median time to progression of 10.5 months. (Fig 6B) (4 vs 10.5, HR 1,86; 95% CI, 1.09-3.16; p=0.023). Due to the small size of our sample and the exploratory nature of this observation, further analyses would be needed. In conclusion, NRF2 overexpression could be associated with worse PFS deriving from platinum-based chemotherapy and trastuzumab in HER2-amplified gastric cancer patients.

Discussion

Although new molecular classifications have been proposed to personalize treatment for GC patients, a precision approach is far from becoming standard. Since HER2 amplification was identified as a target, anti-HER2 drugs have been tested and trastuzumab in combination with platinum based chemotherapy represents the standard of care (4). Nevertheless, primary and acquired resistance to anti-HER2 treatments are frequent events. Unlike the results obtained in HER2-amplified breast cancer, no other anti-HER2 agents used in first-line treatment or beyond progression led to clinical benefit (6-9). Several causes have been proposed to justify the lack of response, such as tumor heterogeneity or molecular characteristics. The heterogeneity of gastric cancer is significant and can limit the use of targeted agents. Molecular changes should also be addressed as responsible for primary or acquired resistance to tailored drugs. Recent data pointed to the *de novo* appearance of *PIK3CA* mutations among GC patients treated with platinum-based chemotherapy and trastuzumab, indicating that hyperactivation of the PI3K/AKT pathway causes acquired resistance (38).

In our study we sought to identify molecular mechanisms responsible for resistance of HER2-amplified GC to anti-HER2 inhibition. We generated both lapatinib- and trastuzumab-stable resistant clones provided by two different HER2-amplified GC cell lines. Both trastuzumab and lapatinib induced activation of the PI3K/AKT/mTOR/RPS6 signaling pathway, in turn sustaining tumor growth and a more aggressive phenotype. The role of RPS6 was stressed. This protein was involved in tumor progression in other solid tumors (39,40). In our work, RPS6 was hyperactivated among all resistant models suggesting its important role in resistance. By silencing RPS6, cell viability significantly decreased. The same result was observed when a PI3K/TORC1/TORC2 inhibitor was used, confirming the implication of the PI3/AKT/mTOR/RPS6 pathway in developing resistance.

A transcriptome analysis performed to better characterize alterations which could cause resistance, found altered gene expression related to response to drugs and metabolic processes. This evidence led to the identification of NRF2 as a crucial point of anti-HER2 resistance in our models. Once activated, NRF2 moves into the nucleus and serves as a master regulator inducing the expression of several cytoprotective genes. Many studies have reported that NRF2 activation in cancer cells promotes cancer progression (41) and metastasis (42), and also confers resistance to chemo and radiotherapy (43). Indeed, lapatinib was shown to induce oxidative stress in breast cancer cells and NRF2 acted to

reduce levels of reactive oxygen species in treated cells (44,45). Moreover, recent reports in lung and pancreatic cancers (12,14-15) have demonstrated that NRF2 promotes metabolic changes able to maintain the aggressiveness of cancer progression (37). In these experiments, NRF2 was also observed to promote cell proliferation under the sustained activation of PI3K/AKT signaling. High NRF2 levels are also known to be associated with poor prognosis in GC (46).

In our *in vitro* model we showed that RPS6 and NRF2 are involved in resistance to anti-HER2 agents. RPS6 was identified as one of the switchers of NRF2, making its activity possible. In a previous report RPS6 was reported to interact with La/SSB, able to bind NRF2 mRNA, inducing an increase of its translation under oxidative stress condition (47). The mechanisms by which these two proteins are related should be further explored. Moreover there is increasing evidence that many aspects of cancer behavior, including treatment sensitivity, depend on post-transcriptional gene regulation (48).

Use of a PI3K/TORC1/TORC2 inhibitor also inhibited RPS6 and consequently NRF2, ultimately decreasing cell viability. When xenografts were generated, a reduction of tumor growth with GSK458, able to decrease both RPS6 and NRF2 activation, suggested the role of these proteins in *in vivo* resistance.

A cohort of HER2-amplified GC patients was also retrospectively analyzed and it was possible to observe NRF2 hyperexpression in patients with poorer PFS. This evidence suggests that NRF2 could be responsible even for primary resistance to anti-HER2 drugs.

In summary, we have shown that NRF2 via RPS6 could be considered as one of the possible mechanism inducing lapatinib and trastuzumab resistance in HER2-amplified GC models *in vitro* and *in vivo.* Beyond genomic changes, such as mutations, post-transcriptional gene regulation should be analyzed as primary determinant of resistance to target agents. RPS6 and NRF2 expression in a cohort of GC patients suggested a trend toward less benefit derived from treatment with trastuzumab. In this scenario, the role of a concomitant treatment with a PI3K/TORC1/TORC2 inhibitor combined with anti-HER2 drugs could be further investigate to evaluate its potential benefit for patients in delaying and/or limiting the emergence of acquired resistance. Although combination therapy has the potential to increase toxicity, it could provide an attractive option in this disease, where resistance will eventually develop. A rationally designed therapeutic strategy as described above could therefore be of interest.

Acknowledgments

The authors thank all the patients who participated in these studies and their families. Special thanks go to Mrs C. Mongort and Dr. S. Navarro from the department of Pathology of the University of Valencia for gathering patient samples and for the IHC assay. The authors thank Dr E. Serna from the Central Unit of Research in Medicine, INCLIVA, Spain, for the assistance with the multigenic analysis.; and Dr A. Diaz for the help with animal care. We would like to thank Dr G. Ayala for the statistical analysis.

This study was supported by grants from the Instituto de Salud Carlos III (Health Institute) (PI18/01909; PI18/01508). VG was funded by an ESMO fellowship program 2014, and holds Rio Hortega contract CM18/00241 from the Carlos III Health Institute; NT was funded by Rio Hortega contract CM15/00246 from the Carlos III Health Institute; DR was

funded by Joan Rodes contract 16/00040 from the Carlos III Health Institute; TF was funded by Joan Rodes contract 17/00026 from the Carlos III Health Institute.

References:

1. Arteaga CL, Engelman JA. ERBB receptors: from oncogene discovery to basic science to mechanism-based cancert herapeutics. *Cancer Cell* **2014**;25:282-303.

2. Moasser MM. The oncogene HER2; Its signaling and transforming functions and its role in human cancer pathogenesis. *Oncogene* **2007**;26:6469-87.

3. Tarazona N, Gambardella V, Huerta M, Roselló S, Cervantes A. Personalised Treatment in Gastric Cancer: Myth or Reality? *Curr Oncol Rep* **2016**;7:18-24.

4. Bang YJ, Van Cutsem E, Feyereislova A, Chung HC, Shen L, Sawaki A, *et al.* Trastuzumab in combination with chemotherapy versus chemotherapy alone for treatment of HER2-positive advanced gastric or gastro-oesophageal junction cancer (ToGA): a phase 3, open-label, randomised controlled trial. *Lancet* **2010**;376: 687-97.

5. Ajani JA, Lee J, Sano T, Janjigian YY, Fan D, Song S. Gastric adenocarcinoma. *Nat Rev Dis* **2017**;3:17036. doi: 10.1038/nrdp.2017.36.

6. Hecht JR, Bang YJ, Qin SK, Chung HC, Xu JM, Park JO, *et al*. Lapatinib in Combination With Capecitabine Plus Oxaliplatin in Human Epidermal Growth Factor Receptor 2-Positive Advanced or Metastatic Gastric, Esophageal, or Gastroesophageal Adenocarcinoma: TRIO-013/LOGiC--A Randomized Phase III Trial. *J Clin Oncol* **2016**;34:443-51.

7. Tabernero J, Hoff PM, Shen L, Ohtsu A, Shah MA, Cheng K, *et al*. Pertuzumab (P) + trastuzumab (H) + chemotherapy (CT) for HER2-positive metastatic gastric or gastro-oesophageal junction cancer (mGC/GEJC): Final analysis of a Phase III study (JACOB). *Ann Oncol* **2017;**28:209-68.

8. Satoh T, Xu RH, Chung HC, Sun GP, Doi T, Xu JM*, et al*. Lapatinib plus paclitaxel versus paclitaxel alone in the second-line treatment of HER2-amplified advanced gastric cancer in Asian populations: TyTAN--A randomized, phase III study. *J Clin Oncol* **2014**;32:2039-49.

9. Thuss-Patience PC, Shah MA, Ohtsu A, Van Custem E, Ajani JA, Castro H, *et al.* Trastuzumab emtansine versus taxane use for previously treated HER2-positive locally advanced or metastatic gastric or gastro-oesophageal junction adenocarcinoma (GATSBY): an international randomised, open-label, adaptive, phase 2/3 study. *Lancet Oncol* **2017**;18:640-53.

10. Bartley AN, Washington MK, Colasacco C, Ventura CB, Ismaila N, Benson AB 3rd, *et al.* HER2 Testing and Clinical Decision Making in Gastroesophageal Adenocarcinoma: Guideline From the College of American Pathologists,American Society for Clinical Pathology, and the American Society of Clinical Oncology. *J Clin Oncol* **2017**;35:N.4.

11. Alsina M, Gullo I, Carneiro F. Intratumoral heterogeneity in gastric cancer: a new challenge to face. *Ann Oncol* **2017**;28:912-13,

12. DeNicola GM, Karreth FA, Humpton TJ, Gopinathan A, Wei C, Frese K, *et al*. Oncogeneinduced Nrf2 transcription promotes ROS detoxification and tumorigenesis. *Nat* **2011**;475:106-9.

13. Rojo de la Vega M, Chapman E, Zhang DD. NRF2 and the Hallmarks of Cancer. *Cancer Cell* **2018**;34:21-43.

14. Best SA, De Souza DP, Kersbergen A, Policheni AN, Dayalan S, Tull D, *et al*. Synergy between the KEAP1/NRF2 and PI3K Pathways Drives Non-Small-Cell Lung Cancer with an Altered Immune Microenvironment. *Cell Metab* **2018**;27:935-43.

15. Chio IIC, Jafarnejad SM, Ponz-Sarvise M, Park Y, Rivera K, Palm W, *et al.* NRF2 Promotes Tumor Maintenance by Modulating mRNA Translation in Pancreatic Cancer. *Cell* **2016**;166:963-76.

16. Jeong Y, Hoang NT, Lovejoy A, Stehr H, Newman AM, Gentles AJ, *et al*. Role of KEAP1/NRF2 and TP53 Mutations in Lung Squamous Cell Carcinoma Development and Radiation Resistance. *Cancer Discov* **2017**;7:86-101.

17. Satoh H, Moriguchi T, Takai J, Ebina M, Yamamoto M. Nrf2 prevents initiation but accelerates progression through the Kras signaling pathway during lung carcinogenesis. *Cancer Res* **2013**;73:4158-68.

18. Kang KA, Piao MJ, Ryu YS, Kang HK, Chang WY, Keum YS, *et al*. Interaction of DNA demethylase and histone methyltransferase upregulates Nrf2 in 5-fluorouracil-resistant colon cancer cells. *Oncotarget* **2016**;26:40594-620.

19. Fan Z, Wirth AK, Chen D, Wruck CJ, Rauh M, Buchfelder M, *et al*. Nrf2-Keap1 pathway promotes cell proliferation and diminishes ferroptosis. *Oncogenesis* **2017**;8:e371.

20. Dai B, Yoo SY, Bartholomeusz G, Graham RA, Majidi M, Yan S, *et al*. KEAP1-dependent synthetic lethality induced by AKT and TXNRD1 inhibitors in lung cancer. *Cancer Res* **2013**;73:5532-43.

21. O'Reilly KE, Rojo F, She QB, Solit D, Mills GB, Smith D, *et al*. mTOR inhibition induces upstream receptor tyrosine kinase signaling and activates Akt. *Cancer Res* **2006**;66:1500-8.

22. Carracedo A, Pandolfi PP. The PTEN–PI3K pathway: of feedbacks and cross-talks. *Oncogene* **2008**;27:5527-41.

23. Bjornsti MA, Houghton PJ. The TOR pathway: a target for cancer therapy. *Nat Rev Cancer* **2004**;4:335-48.

24. Karlsson E, Pérez-Tenorino G, Amin R, Bostner J, Skoog L, Fornander T, *et al*. The mTOR effectors 4EBP1 and S6K2 are frequently coexpressed, and associated with a poor prognosis and endocrine resistance in breast cancer: a retrospective study including patients from the randomised Stockholm tamoxifen trials. *Breast Cancer Res* **2013**;15:R96.

25. Xie X, Guo P, Yu H, Wang Y, Chen G. Ribosomal proteins: insight into molecular roles and functions in hepatocellular carcinoma. *Oncogene* **2018**;37:277-85.

26. Roux PP, Shahbazian D, Vu H, Holz MK, Cohen MS, Taunton J, *et al*. RAS/ERK Signaling Promotes Site-specific Ribosomal Protein S6 Phosphorylation via RSK and Stimulates Cap-dependent Translation. *J Biol Chem* **2007**;282:14056-64.

27. Mendoza MC, Er EE, Blenis J. The Ras-ERK and PI3K-mTOR Pathways: Cross-talk and Compensation. *Trends Biochem Sci* **2011**;36:320-28.

28. Pavlova NN, Thompson CB. The emerging hallmarks of cancer metabolism. *Cell metab* **2016**;23:27-47.

29. Sanchez-Vega F, Mina M, Armenia J, Chatila WK, Luna A, La KC, *et al*. Oncogenic signaling pathways in the cancer genome atlas. *Cell* **2018**;173:321–37.

30. Basak P, Sadhukhan P, Sarkar P, Sil PC. Perspectives of the Nrf-2 signaling pathway in cancer progression and therapy. *Toxicol Rep* **2017**;4:306-18.

31. Riffo-Campos A, Gimeno-Valiente F, Rodriguez FM, Cervantes A, Lopez-Rodas G, Franco L, *et al*. Role of epigenetic factors in the selection of the alternative splicing isoforms of human *KRAS* in colorectal cancer cell lines. *Oncotarget* **2018**;9:20578-89.

32. Wang X, Spandidos A, Wang H, Seed B. PrimerBank: a PCR primer database for quantitative gene expression analysis, 2012 update. *Nucleic Acids Res* **2012**;40:D1144-9.

33. Kim SH, Jang YH, Chau GC, Pyo S, Um SH. Prognostic significance and function of phosphorylated ribosomal protein S6 in esophageal squamous cell carcinoma. *Mod Pathol* **2013**;26:327-35.

34. Chen B, Zhang W, Gao J, Chen H, Jiang L, Liu D, *et al*. Downregulation of ribosomal protein S6 inhibits the growth of non-small cell lung cancer by inducing cell cycle arrest, rather than apoptosis. *Cancer Lett* **2014**; 354:378-89.
35. Kawasaki Y, Ishigami S, Arigami T, Uenosono Y, Yanagita S, Uchikado Y, *et al*. Clinicopathological significance of nuclear factor (erythroid-2)-related factor 2 (Nrf2) expression in gastric cancer. *BMC Cancer* 2015;15:5. doi: 10.1186/s12885-015-1008-4.

36. Tong Y, Zhang B, Yan YY, Fan Y, Yu J, Kong SS, *et al*. NRF2 NSCLC Dual-negative expression of Nrf2 and NQO1 predicts superior outcomes in patients with non-small cell lung cancer. *Oncotarget* **2017**;8:45750-58.

37. Wang H, Liu X, Long M, Huang Y, Zhang L, Zhang R, *et al*. NRF2 activation by antioxidant antidiabetic agents accelerates tumor metastasis. *Sci Transl Med* **2016**;8:334ra51.

38. Pietrantonio F, Fucà G, Morano F, Gloghini A, Corso S, Aprile G, *et al*. Biomarkers of primary resistance to trastuzumab in HER2-positive metastatic gastric cancer patients: the AMNESIA case-control study. *Clin Cancer Res* **2018**;24:1082-89.

39. Khalaileh A, Dreazen A, Khatib A, Apel R, Swisa A, Kidess-Bassir N, *et al*. Phosphorylation of ribosomal protein S6 attenuates DNA damage and tumor suppression during development of pancreatic cancer. *Cancer Res* **2013**;73:1811-20.

40. Chen B, Tan Z, Gao J, Wu W, Liu L, Jin W, *et al*. Hyperphosphorylation of ribosomal protein S6 predicts unfavorable clinical survival in non-small cell lung cancer. *J Exp Clin Cancer Res* **2015**;34:126.

41. Tao S, Rojo de la Vega M, Chapman E, Ooi A, Zhang D.D. The effects of NRF2 modulation on the initiation and progression of chemically and genetically induced lung cancer. *Mol Carcinog* **2017**;57:182-92.

42. Chang CW, Chen YS, Tsay YG, Han CL, Chen YJ, Yang CC, *et al*. ROS-independent ER stress-mediated NRF2 activation promotes warburg effect to maintainstemness-associated properties of cancer-initiating cells. *Cell Death Dis* **2018**;9:194. doi: 10.1038/s41419-017-0250-x.

43. Wang H, Liu X, Long M, Huang Y, Zhang L, Zhang R, *et al*. NRF2 activation by antioxidant antidiabetic agents accelerates tumor metastasis. *Sci Transl Med* 2016;8:334ra51.

44. Wu T, Harder BG, Wong PK, Lang JE, Zhang DD. Oxidative Stress, Mammospheres and Nrf2 – New Implication for Breast Cancer Therapy? *Molecular carcinogenesis*. 2015;54(11):1494-1502. doi:10.1002/mc.22202.

45. Zhang, R., Qiao, H., Chen, S., Chen, X., Dou, K., Wei, L., & Zhang, J. (2016). Berberine reverses lapatinib resistance of HER2-positive breast cancer cells by increasing the level of ROS. *Cancer Biology & Therapy*, *17*(9), 925–934. http://doi.org/10.1080/15384047.2016.1210728

46. Yu S, Wu T, Wang J, Cheng C, Wang J, Sun L,. Combined Evaluation of Expression of CXCR4 and Nrf2 as Prognostic Factor for Patients with Gastric Carcinoma. *Anticancer Agents Med Chem*. **2018**;18(3):388-393.

47. Zhang J, Dinh TN, Kappeler K, Tsaprailis G, Chen QM. La autoantigen mediates oxidant induced de novo Nrf2 protein translation. *Mol Cell Proteomics* **2012**;11:M111.015032.

48. Blagden SP, Willis AE.The biological and therapeutic relevance of mRNA translation in cancer. *Nat Rev Clin Oncol* **2011**;8:280-91

Figures legends:

Figure1.

Viability and changes in protein expression in lapatinib-resistant models. **A,** Viability according to increasing doses of lapatinib of OE19 cell line and its resistant clones, LR1OE and LR2OE. The IC_{50} obtained were respectively 0.17μM for OE 19; 0.56μM for LR1OE and 0.61μM for LR2OE.

B, Analysis of whole-cell protein extracts of OE19, LR1OE and LR2OE-resistant clones by human Phospho-RTK signaling antibody array. Hotspots of phosphorylated proteins are highlighted. **C,** Representative images of Western Blot analysis of different proteins expression and activation among OE19 and the resistant lines, LR1OE and LR2OE, with the indicated antibodies.

Figure2.

Transcriptomic assay suggested NRF2 to be involved in lapatinib resistance. **A,** PCA analysis showing mRNA expression profiles of OE19 and LR1OE and LR2OE. The ellipsoids show a different directionality in each cell line based on gene expression. **B,** Heat map of the expression profile changes between OE19 and its derived lapatinib-resistant cell lines. The expression scale is shown under the heat map. Blue boxes represent low expression and red high expression. **C,** Functional annotation of genes using Pathway Studio database. Pie charts represent the percentage of significantly enriched biological processes. **D**, Volcano plot showing statistical significance (p-value (-Log base10)) against fold change (log) of gene expression changes between OE19 and LR1OE cell lines. Arrows indicate genes which were statistically differentiated and recognized to be targets of NRF2. Dotted lines indicate the limit of a p value of 0.05 and a fold change of 2. **E,** Changes in mRNA expression of NRF2 targets identified in microarray assay analyzed by RT-qPCR. Representation of P value: *, < 0.05; **< 0.01; *** < 0.001. **F,** Representative images of Western Blot analysis of NRF2 expression among OE19, LR1OE and LR2OE with the indicated antibodies.

Figure3.

NRF2 and RPS6 activation as anti-HER2 drug resistant factors across different models. **A,** Viability of NCI-N87 cell line and its resistant clones, LR1NCI and TR1NCI, to increasing doses of lapatinib and trastuzumab, respectively. When lapatinib was administered, the IC_{50} obtained was respectively $4.4x10^{-4}$μM for NCI-N87 and $2.3x10^{-2}$μM for LRNCI. When trastuzumab was used, IC_{50} were respectively 10μg/ml for NCI-N87 and >1000 for TRNCI. **B,** Western Blot analysis of different proteins expression and activation of NCI-N87 and the resistant lines LR1NCI and TR1NCI with the indicated antibodies. **C,** Western Blot analysis of NRF2 expression of NCI-N87 and the derived resistant lines. **D,** Representative images of NRF2 expression analyzed by immunofluorescence with a confocal microscope in the cell lines indicated. Cells were contrasted with DAPI (blue) for visualization of the nuclei.

Figure4.

Inhibition of RPS6 activation by GSK458, a PI3K/TORC1/TOC2 inhibitor, or by siRNAs decreases viability across all resistant models. The concomitant decrease of NRF2 expression in LR1OE cells is shown. Representation of P value: *< 0.05; **< 0.01; *** < 0.001. **A,** Effect of a selected targeted agents on cell viability across different resistant models (OE19 on the left; NCI-N87 on the right). Cell viability was evaluated versus vehicle-treated cells after 72 h. **B,** Effect of RPS6 knockdown on cell proliferation across different resistant models (OE19 on the left and NCI-N87 on the right). Viable cells were measured at 48 and 96 h after siRNA transfection with RPS6 siRNA (siRPS6) or siRNA control (siC). **C,** Viability of RPS6 knockdown cells exposed to different doses of lapatinib or trastuzumab versus vehicle-treated cells (OE19 model, on the left; NCI-N87 lapatinib-resistant model, in the middle; and NCI-N87 trastuzumab-resistant model, on the right). **D,** Western blot analysis of RPS6 and NRF2 protein expression and quantification in LR1OE cell line (left). Whole protein lysates obtained from non-transfected cells and 72h after transfection with siC or siRPS6 were used. Changes in mRNA expression of some NRF2 targets after *RPS6* knockdown compared with siC transfected cells analyzed by RT-qPCR (right). **E,** Effect of *NRF2* knockdown on proliferation of OE19 and LR1OE cell lines. Cells were transfected with *NRF2* siRNAs (siNRF2) or control siRNAs (siC) and number of cells were measured at 48 and 96 h after silencing. **F**, Viability of NFR2 knockdown cells exposed to different doses of lapatinib or trastuzumab versus vehicle-treated cells (OE19 model, on the left; NCI-N87 trastuzumab-resistant model, on the right). **G,** LR1OE cell lines were treated with vehicle or different targeted drugs for 8 h. Whole cell extracts were subjected to immunoblotting with the indicated antibodies. NRF2 and RPS6 protein bands were quantify using imageJ program (right).

Figure5.
PI3K/TORC1/TORC2 inhibitor, GSK458, decreased pRPS6 and NRF2 expression, as well as reducing tumor growth *in vivo.* **A,** Tumor volume of mice bearing LR1OE cells treated with vehicle (control), lapatinib or lapatinib/GSK458 for 15 days. **B,** Tumor size at sacrifice. **C,** Representative Western blot analysis of whole protein extracts of tumors at sacrifice with the indicated antibodies. **D,** Changes in mRNA expression of NRF2 targets of LR1OE xenograft tumors after different mice treatments analyzed by RT-qPCR**.** Representation of P value: * < 0.05; ** < 0.01; *** < 0.001.

Figure6.
Analysis of NRF2 expression and resistance to trastuzumab and platinum-based chemotherapy in a cohort of HER2-amplified locally advanced or metastatic GC patients. **A,** Example of IHC staining according to low or high RPS6 expression and low or high NRF2 expression in tumor samples derived from HER2-amplified GC patients. **B,** Time to progression of patient analyzed according to different NRF2 expression (High versus Low). Kaplan Meier curves.

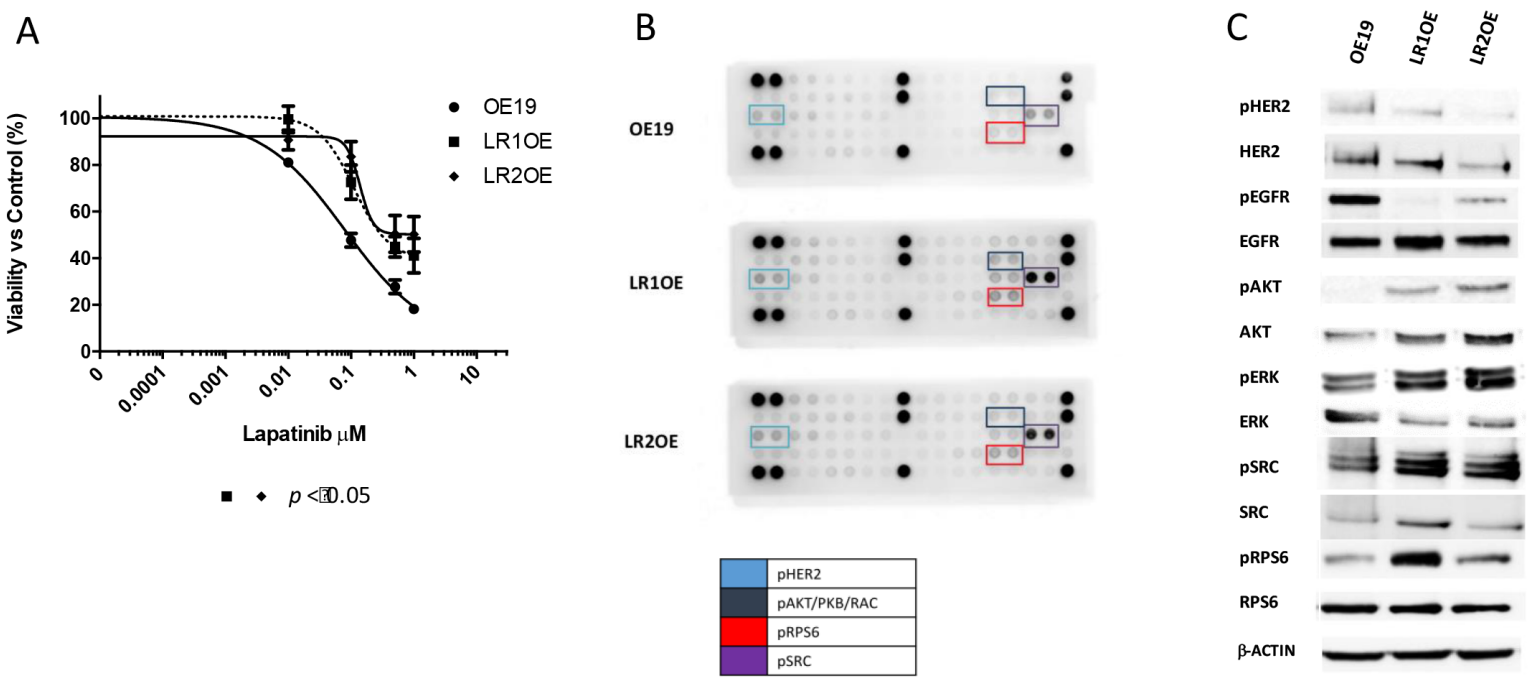

Figure 1.

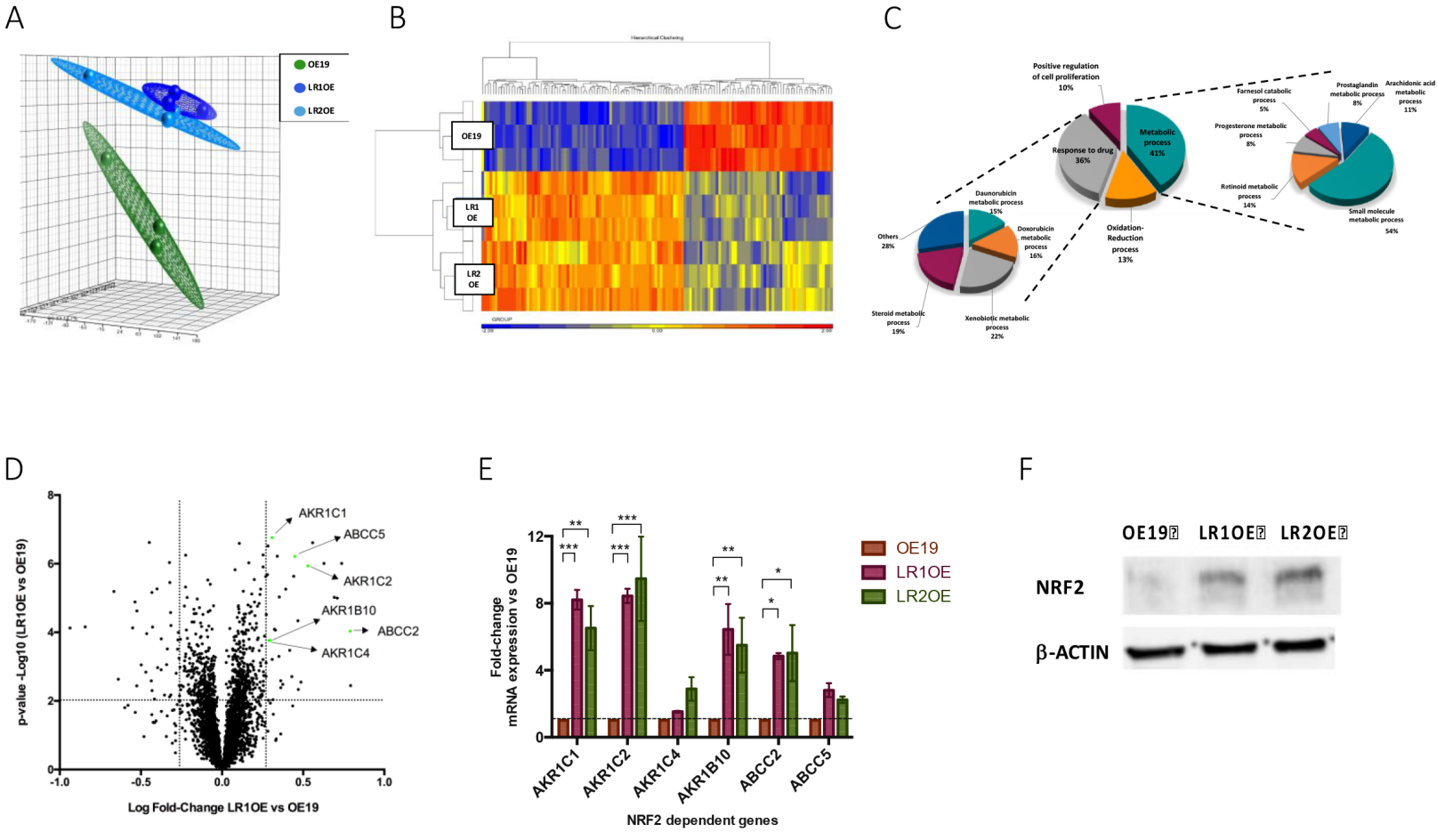

Figure 2.

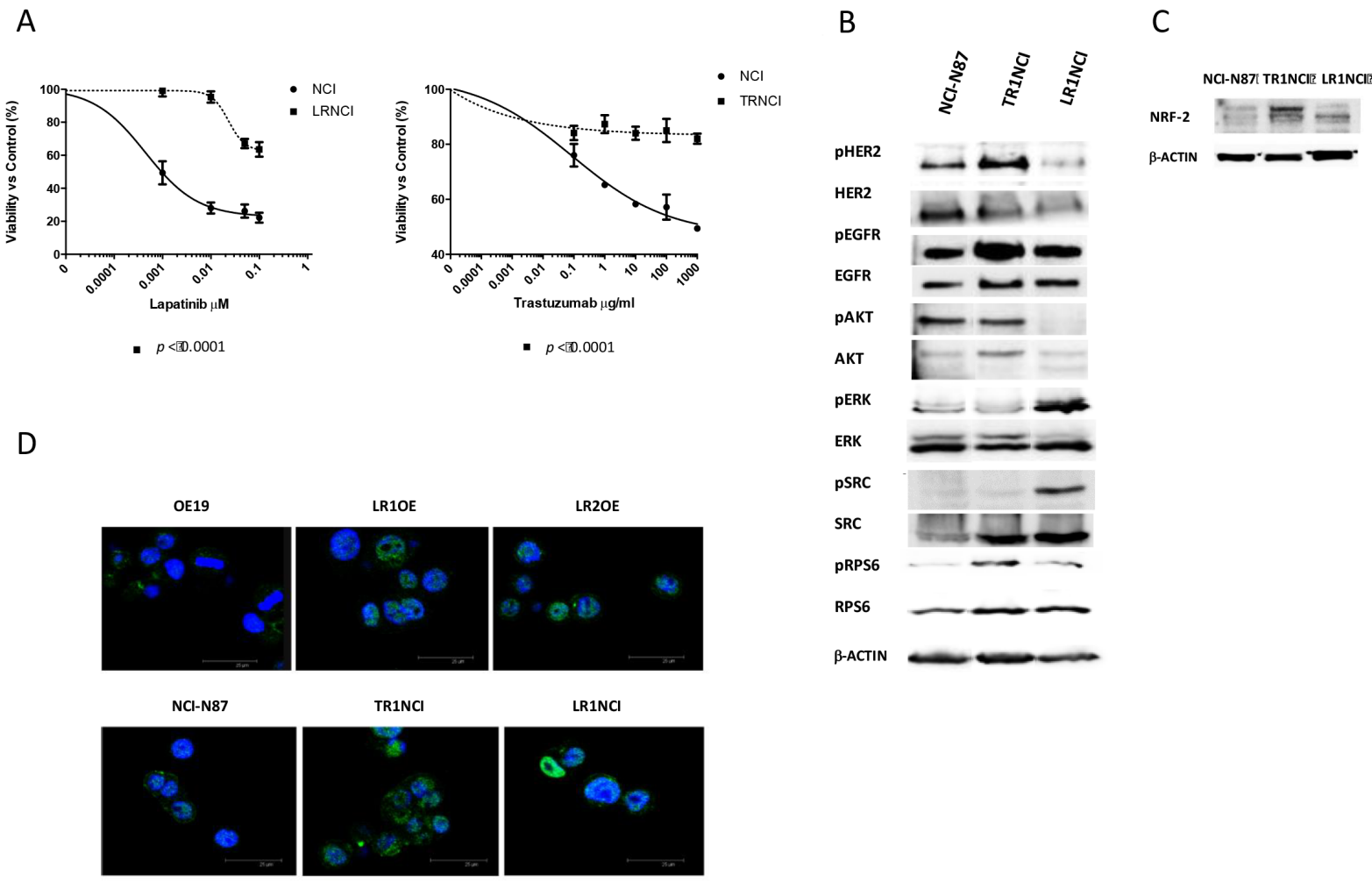

Figure 3.

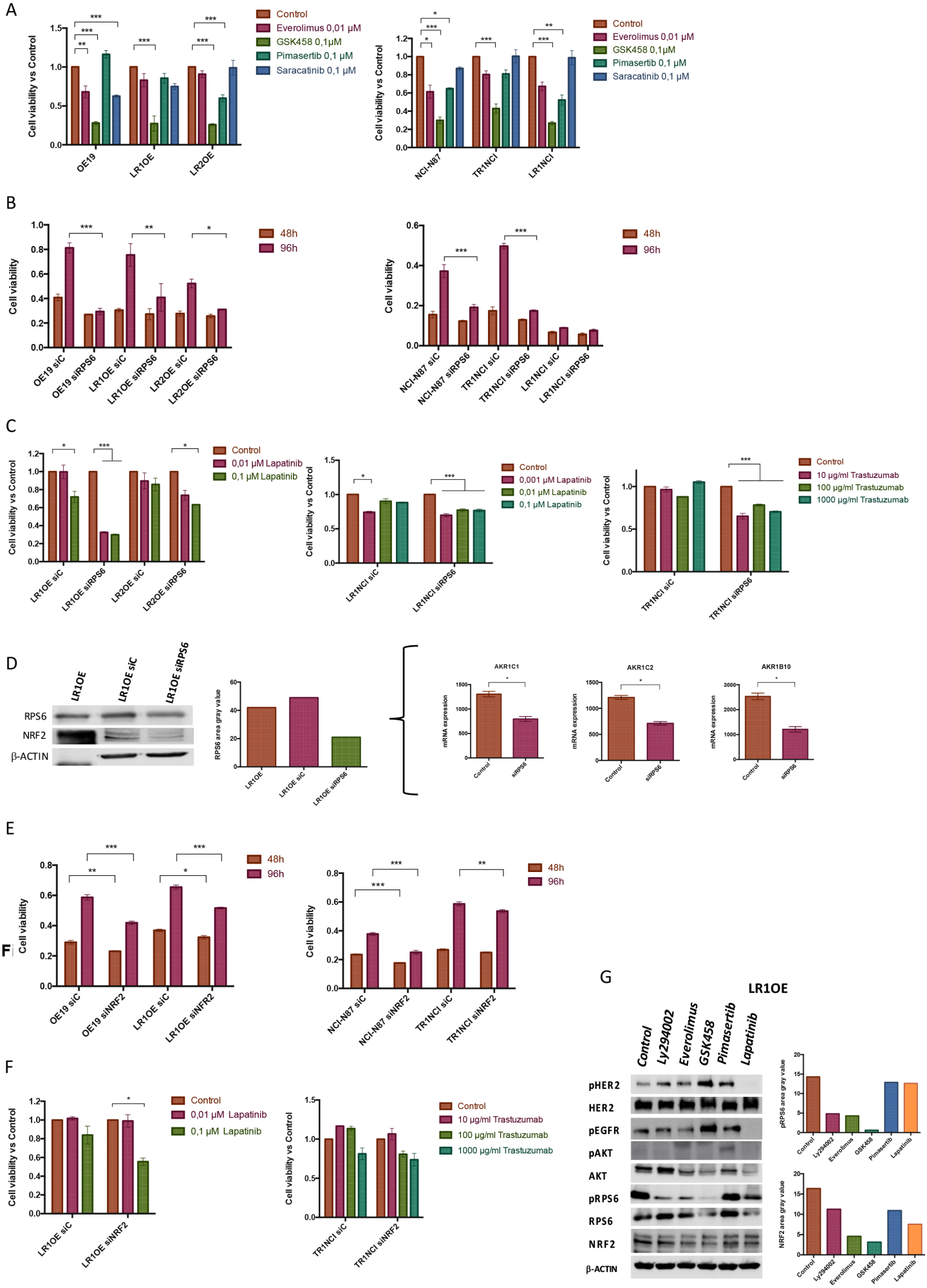

Figure 4.

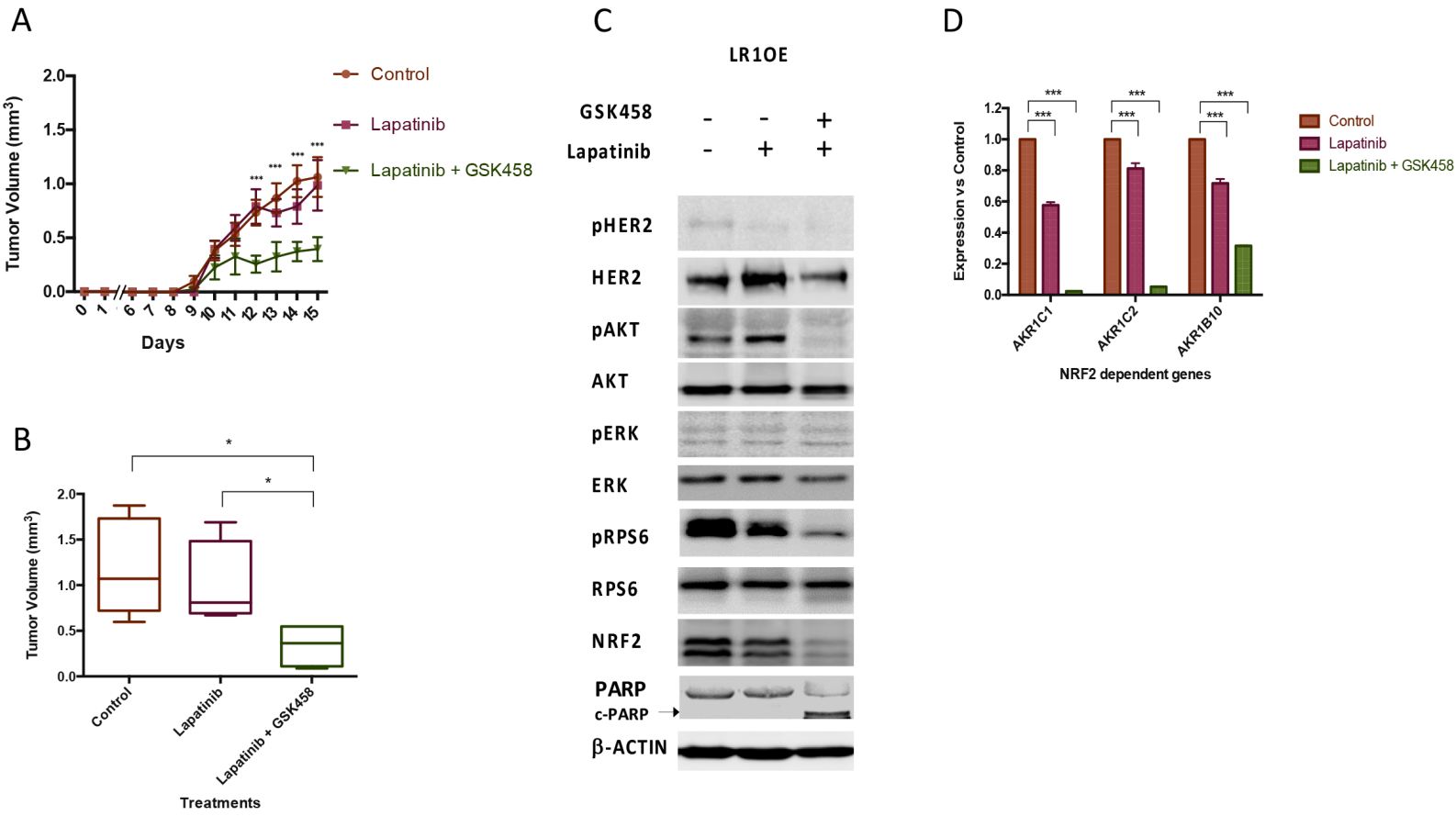

Figure 5.

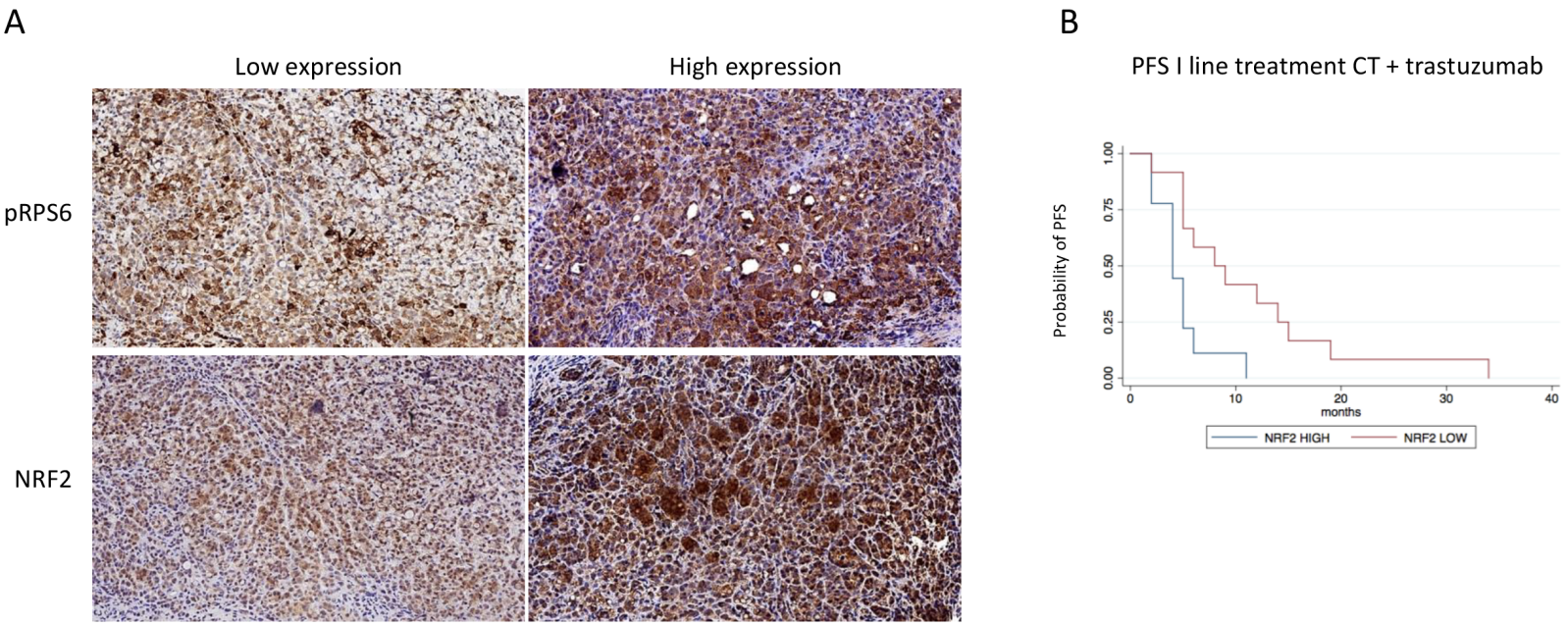

Figure 6.

AACR American Association for Cancer Research

Clinical Cancer Research

NRF2 through RPS6 activation is related to anti-HER2 drug resistance in HER2-amplified gastric cancer

Valentina Gambardella, Francisco Gimeno-Valiente, Noelia Tarazona, et al.

Clin Cancer Res Published OnlineFirst November 30, 2018.